Bull. Mater. Sci., Vol. 34, No. 4, July 2011, pp. 811–814. © Indian Academy of Sciences.

High temperature oxidation of Ti–48Al–8Cr–2Ag alloy with sputtered coating at 1000°C in air

Y J XI* and Y J LIU

School of Materials and Chemical Engineering, Zhongyuan University of Technology, Zhengzhou 450007, P.R. China

MS received 31 August 2009; revised 5 March 2010

Abstract. Magnetron-sputter deposition was used to produce a Ti–48Al–8Cr–2Ag (at.%) coating on a cast alloy substrate with the same composition. The oxidation behaviour of the cast Ti–48Al–8Cr–2Ag alloy and its sputtered coating was investigated in air at 1000°C. The resulting scale structures were analyzed in great detail by scanning electron microscopy (SEM) and transmission electron microscopy (TEM). The nanocrystalline coating showed higher oxidation rate than the cast alloy, because an outer TiO_2 layer formed over a fine-grain Al_2O_3 scale on the coating. The oxidation mechanism was discussed.

Keywords. Ti–Al–Cr–Ag nanocrystalline coating; high temperature oxidation.

1. Introduction

There is an increasing interest in γ-TiAl based alloys from a technical point of view because of their light weight and their remarkable high-temperature strength, suggesting their use in gas turbines and as parts in automotive engines (Kim 1989; Luthra 1991; Kim 1995). However, the poor oxidation resistance of TiAl must be overcome before it can be used at an elevated temperature because it does not form a continuous Al_2O_3 scale, but a non-protective $TiO_2 + Al_2O_3$ mixed scale (Becker *et al* 1992; Dettenwanger *et al* 1998).

In order to enhance the oxidation resistance of TiAl-base intermetallics, several kinds of coatings have been investigated (Wang *et al* 1995; Nishimoto *et al* 2003; Marie-Pierre *et al* 2003; Xiang *et al* 2003; Fukumoto *et al* 2004; Zhu *et al* 2007; Xiong *et al* 2008). A new class of Ti–Al–Cr coatings has been proposed and they provided excellent protection for TiAl intermetallics (Brady *et al* 1997a, b; Tang *et al* 2003; Xi *et al* 2004; Tang *et al* 1997). Tang *et al* (1997) reported that the Ti–50Al–10Cr coating provided excellent protective for the TiAl alloy. However, many of the oxidation resistance compositions tend to be very brittle thus degrading mechanical properties. Ag-containing alloys can show excellent mechanism property (Shemet *et al* 2000). Ag can stabilize the Z-phase ($Ti_5Al_3O_2$) in the subscale-depletion layer thereby preventing formation of α_2-Ti_3Al as well as Ti-rich nitrides (Shemet *et al* 2000; Tang *et al* 2003), which were responsible for the destruction of alumina scales in common γ-TiAl alloys. In addition, Ag is needed to improve mechanical properties.

In order to keep the capability of protective Al_2O_3 formation, a high Cr content and Ag addition is necessary. A series of TiAl alloys with Cr and Ag addition was investigated, and Ti–Al–Cr–Ag also exhibited excellent oxidation resistance (Tang *et al* 2003; Xi *et al* 2004). Therefore, some researchers believe that Ti–Al–Cr–Ag coatings may become a promising protective coating for TiAl-base intermetallics. This predictive result is based on macrostructure of oxide scale of Ti–Al–Cr–Ag coating. Investigation roughly may lead to a one-sided view. Therefore, it is necessary to further study the oxidation of Ti–Al–Cr–Ag (at.%) coating in more detail by means of TEM to clearly understand the oxidation process, about which no data has been reported. In the present study, oxidation behaviour of Ti-48Al–8Cr–2Ag (at.%) coating on the same substrate was studied using TEM to reveal oxidation mechanics.

2. Experimental

The alloy investigated was Ti–48Al–8Cr–2Ag (at.%). The resulting microstructure was γ-TiAl and Laves phase. The Ti–48Al–8Cr–2Ag coating was prepared by magnetron sputtering technique. The target of $380 \times 126 \times 7$ mm and the specimens of $10 \times 10 \times 2{\cdot}5$ mm were cut from an alloy ingot. The specimens were ground down to No. 600 emery paper, peened and ultrasonically cleaned in ethanol. The peening treatment was to improve the adhesive energy. The deposition procedure and the morphology and microstructure of the coating are narrated in detail elsewhere (Xi *et al* 2004). Energy dispersive X-ray

*Author for correspondence (yjxi@sina.com)

(EDX) showed that the coating had an approximate composition of Ti–46·2Al–7·7Cr–1·7Ag, a composition similar to the Ti–48Al–8Cr–2Ag alloy. Isothermal oxidation test was carried out at 1000°C in air. An electronic thermal balance was used to monitor the mass change continuously.

The specimens were analysed using SEM, EDX and TEM. For the preparation of cross-sectional TEM specimens, the oxidized sample was sectioned by a diamond saw into disks with thickness of around 500 μm in order to get a cross-section of oxide scale. Then two disk samples were glued with the oxide scale face-to-face. After that the disks were mechanically ground to a thickness of 50 μm. To reduce the thickness of the sample further, dimples were made on each side of the disk by a dimple grinder. The samples were then thinned to electron transparency using ion-beam milling. The acceleration voltage of the argon ions used was 4–5 kV, the gun current was 0·8 mA, and the thinning angle varied from 15–7°.

3. Results

3.1 *Oxidation kinetics*

Figure 1 shows the isothermal oxidation kinetics of the alloy and its coating. Ti–48Al–8Cr–2Ag (at.%) alloy and its coating exhibited low oxidation rate at 1000°C. Parabolic rate constants, K_p, were calculated by plotting (weight gain)^2 vs time. Parabolic rate constants for oxidation of the cast alloy and nanocrystalline coating at 1000°C are $8{\cdot}24 \times 10^{-4}$ and $2{\cdot}04 \times 10^{-3}$ mg^2/cm^4 h^{-1} respectively. At the beginning of oxidation a strong increase in weight can be observed for the nanocrystalline coating. It was interesting to note that the parabolic rate constant of cast alloy with coating at 1000°C was higher than that of the cast alloy.

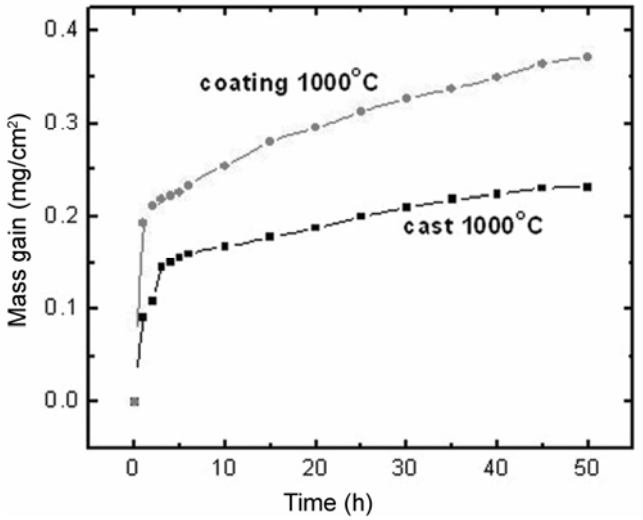

Figure 1. Isothermal oxidation kinetics of specimens at 1000°C.

3.2 *SEM and TEM investigations of specimens*

Figures 2 and 3 show the cross-sectional microstructures of cast alloy and the coating at 1000°C, respectively. Cast alloy and its coating formed a thin scale. It was very difficult to identify the phase in the scale clearly. After oxidation at 1000°C the Al_2O_3 scale was very adherent and was less than 2 μm on the cast alloy. Beneath the oxide scale, an almost continuous zone of Al-depletion mainly consisting of $Ti(Cr,Al)_2$ laves phase was present.

In order to investigate the oxide scale in further detail, a cross-sectional TEM specimen was prepared. Figures 4 and 5 show cross-sectional micrographs and SAD patterns corresponding to the scale on Ti–48Al–8Cr–2Ag (at.%) alloy and the coating after oxidation at 1000°C in air respectively. The cast alloy formed a scale of only Al_2O_3, as shown in the TEM bright-field image of figure 4.

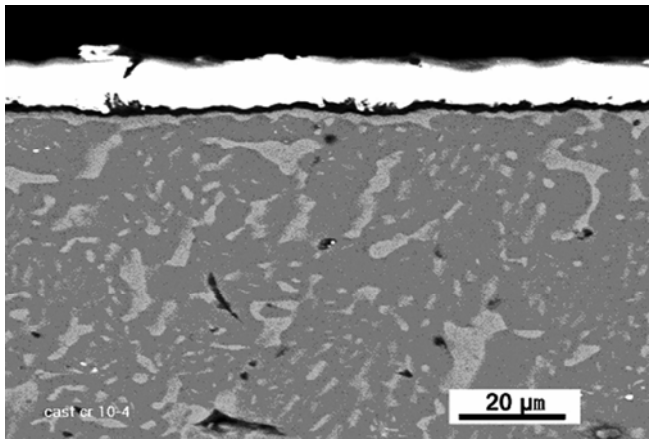

Figure 2. Cross-sectional microstructure of the cast alloy after 50 h oxidation at 1000°C.

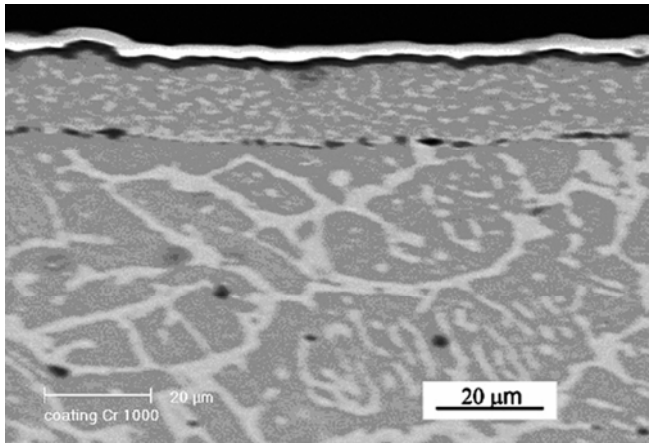

Figure 3. Cross-sectional microstructure of the coating after 50 h oxidation at 1000°C.

SAD showed that the X-phase formed beneath the Al_2O_3 scale. The phenomena that occurred on the coating was different from that on the cast alloy. An outer TiO_2 layer formed above the fine-grain Al_2O_3 layer on the coating after oxidation, as shown in the TEM bright-field image and corresponding SAD patterns of figure 5.

4. Discussion

The high temperature oxidation resistance of Ti–Al–Cr–Ag alloy was dependent on the formation of protective Al_2O_3 scale. In the present study, protective Al_2O_3 scale formed on the cast alloy after 50 h oxidation because of Cr and Ag addition. Brady *et al* (1997a, b) found that substitution of Cr for Ti in Ti–Al for more than 8–10 at.% can reduce the level of Al needed for protective Al_2O_3 scale formation during oxidation. Laves phase possesses much higher Cr than the Ti–Al-phase, which also exhibited beneficial effect on Al_2O_3 formation. Ag can stabilize the X-phase ($Ti_5Al_3O_2$) in the subscale-depletion layer thereby preventing formation of Ti_3Al (Shemet *et al* 2000; Tang *et al* 2003), which is another reason for Al_2O_3 scale formation. X-phase beneath the Al_2O_3 scale in figure 4 also confirmed this result.

Although some studies showed similar oxidation kinetics of Ti–Al–Cr–Ag alloy and its coating, analysis of cross-sectional microstructures was different. The nanocrystalline Ti–48Al–8Cr–2Ag (at.%) coating oxidized more rapidly than the cast alloy at 1000°C from the oxidation kinetics. SEM and TEM analysis of the cross-sectional structure showed that only a Al_2O_3 scale formed on the cast alloy while an outer TiO_2 layer formed over a fine-grain Al_2O_3 layer on the coating after oxidation. Some researchers focused on macrostructure of oxide scale of Ti–Al–Cr–Ag coating or Ti–Al–Cr coating. They observed that only Al_2O_3 scale formed on both the coating and the cast alloy after oxidation at 1000°C. They believed that the coating exhibited higher oxidation rate than the cast alloy since the coating possessed a rougher surface, which resulted from a shadowing effect (Lou *et al* 1995; Yang *et al* 2002). In fact, besides the rougher surface, the outer TiO_2 layer formation was another important factor resulting in the higher oxidation rate of the coating. TiO_2 scale formation on the coating was not related to Ag element because the coating exhibited a similar composition to the substrate. Oxidation of Ti was accompanied by increasing scale growth rate. The standard Gibbs free energy of Ti conversion to TiO_2 at 1000°C was about –715·51 kJ/mol, while the standard Gibbs free energy of Al conversion to Al_2O_3 was about –636·89 kJ/mol, therefore TiO_2 grew faster than Al_2O_3. The coarse TiO_2 layer cannot create a continuous, adherent, non-porous protective layer that prevents further oxidation (Kim 1989, 1995; Luthra 1991). In addition, TiO_2 formed on the coating partly because of the effect of grain size reduction. Grain size reduction not only enhanced the diffusivities of Al but also the diffusivities of Ti as a result of grain-boundary diffusion.

5. Conclusions

(I) The nanocrystalline Ti–48Al–8Cr–2Ag (at.%) coating showed higher oxidation rate than the cast alloy at 1000°C.

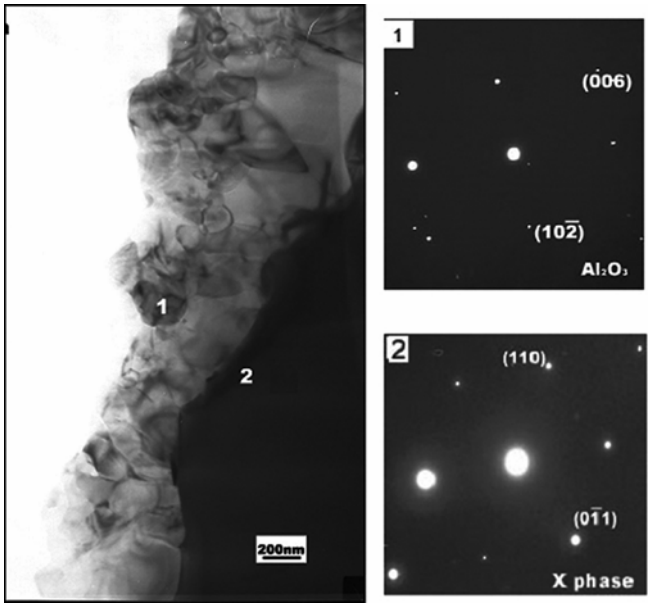

Figure 4. Cross-sectional TEM micrograph of Ti–48Al–8Cr–2Ag (at.%) alloy after oxidation for 50 h at 1000°C in air, and SAD patterns corresponding to areas '1' and '2'.

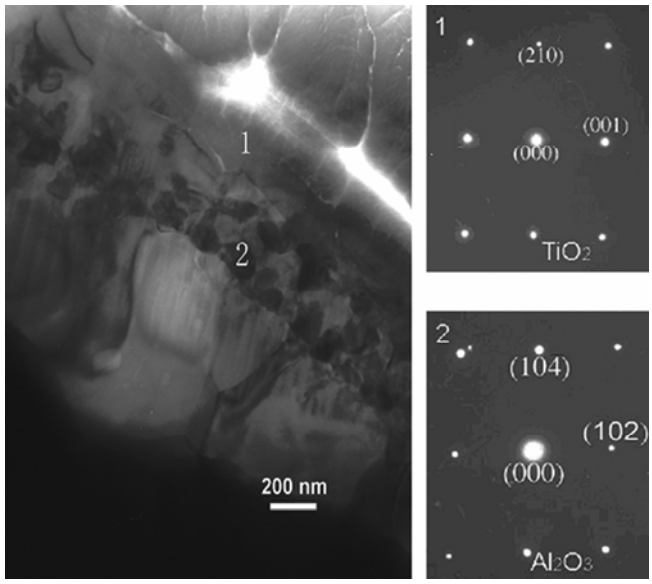

Figure 5. Cross-sectional TEM micrograph of the alloy sputtered with nanocrystallline coating after oxidation for 50 h at 1000°C in air, and SAD patterns corresponding to areas '1' and '2'.

(II) After thermal oxidation at 1000°C, only a Al_2O_3 scale formed on the cast alloy, while an outer TiO_2 layer formed over a fine-grain Al_2O_3 scale on the coating, which is one of the most important factors leading to the faster oxidation rate of the coating.
(III) Grain size reduction was another important reason for high oxidation rate of the nanocrystalline Ti–48Al–8Cr–2Ag (at.%) coating.
(IV) Whether Ti–Al–Cr–Ag can be a promising coating for TiAl alloy or not must be studied in further detail.

References·

Becker S, Rahmel A and Schorr M 1992 *Oxid Met.* **38** 425
Brady M P, Smialke J L and Humphray D L 1997a *Acta Metall. Meter.* **45** 2371
Brady M P, Smialke J L and Smith J 1997b *Acta Metall. Meter.* **45** 2357
Dettenwanger F, Schumann E, Ruhle M, Rakowski J and Meier G H 1998 *Oxid Met.* **50** 269
Fukumoto M, Hara M and Nagataki T 2004 *Oxid. Met.* **61** 1
Kim Y M 1989 *J. Met.* **42** 24
Kim Y M 1995 *J. Met.* **47** 38
Lou H Y, Zhu S L and Wang F H 1995 *Oxid. Met.* **48** 317
Luthra K L 1991 *Oxid.Met.* **36** 475
Marie-Pierre B, Benoit G and Pieere J 2003 *Surf. Coat. Technol.* **162** 248
Nishimoto T, Izumi T, Shigenari and Natta T 2003 *Intermetallics* **11** 225
Shemet V, Tyagi A K and Becker J S 2000 *Oxid. Met.* **54** 211
Tang Z, Shemet V, Niewolak L and Quadakkers W J 2003 *Intermetallics* **11** 1
Tang Z, Wang F H and Wu W T 1997 *Oxid. Met* **48** 511
Wang F H, Lou H Y and Wu W T 1995 *Oxid. Met.* **43** 395
Xiang Z D, Rose S R and Datta P K 2003 *Mater Chem. Philos.* **80** 482
Xiong YM, Zhu S L, Wang F H and Lee C H 2008 *Coat .Technol. Res.* **5** 93
Xi Y J, Wang F H and He L L 2004 *Mater. Sci. Forum* **461** 1181
Yang S L, Wang F H, Sun Z M and Zhu S L 2002 *Intermetallics* **10** 467
Zhu M, Li M S, Duo S W and Zhou Y C 2007 *J. Mater. Sci. Technol.* **A23** 373